Second International Symposium on Marine Propulsors
smp'11, Hamburg, Germany, June 2011
Workshop: Propeller performance

Open Water Test Propeller Performance and Cavitation Behaviour using PPB and FreSCo$^+$

Scott Gatchell, Dieke Hafermann, Heinrich Streckwall[1]

[1]Hamburg ship Model Basin (HSVA), Hamburg, Germany

ABSTRACT

To generate the requested results for the SMP 11 propeller workshop HSVA applied three in-house codes, namely the Panel code 'PPB', the Vortex Lattice Method 'QCM' and RANS solver 'FreSCo' computations.

Keywords

RANS code FreSCo$^+$, Panel Code PPB, Vortex-Lattice Code QCM

1 INTRODUCTION

All three codes ('PPB', 'QCM' and 'FreSCo') were applied for the open water diagram (case 2-1). Two codes, 'PPB' and 'FreSCo', were able to produce results for the propeller slipstream structure at 0.1D and 0.2D behind the generator line (case 2-2). The cavitation behavior was estimated by 'QCM' and 'TreSCo' (case 2-3).

2 NUMERICAL METHOD

2.1 PPB

The program system 'PPB' serves to analyze marine propellers using a surface panel method. The method is 'potential based', meaning that the basic unknown related to each individual surface element is the local perturbation potential. As all elements together represent the blade surface, in the first solution step one obtains the flow potential on the complete blade and –if modeled – also on the hub. Further evaluation of surface values of the flow potential give surface pressures and overall forces. Viscous corrections entering the open water performance are as well based on the complete panel system, summing shear force contributions from each element, whereby local shear is estimated from flat plate friction lines. The slipstream analysis is an option, requiring Velocity 'sensors' behind the propeller. Practically this options is used as the first step of a fast rudder analysis, also based on a surface panel method.

2.2 QCM

The program system 'QCM' uses the camber surface to represent the propeller blade. The basic elements are discrete line vortices combined with suitably located control points. Obeying Helmholtz's second theorem (addressing the vortex filament behavior) the complex vortex structure related to one blade, including the complete trailing vortex system, can be cut down to a small number of unknowns, the so called 'bound' vortex elements. For the surface pressure calculation, discrete vortices are 'smeared' to give surface vorticity, the latter describing the velocity jump across the camber surface. This information allows to derive the surface pressure. A cavity model may be run as an add on analysis, manipulating the fully wetted pressure via additional singularities until constant pressure in cavitating zones is reached.

2.3 RANS computations: FreSCo$^+$

The FreSCo$^+$ code solves the incompressible, unsteady Navier-Stokes-equations (RANS) (Hafermann 2007). The transport equations are discretized with the cell-centered finite volume method. The code can use unstructured grids from different grid generators such as the fully unstructured, automatic grid generator HEXPRESS. This reduces the time needed for generating typical grids from several days down to several hours. The governing equations are solved in a segregated manner, utilizing a volume-specific pressure correction scheme to satisfy the continuity equation (Ferziger and Peric, 2002). To avoid an odd-even decoupling of pressure and velocity, a third-order pressure smoothing is employed along the way which is outlined by Rhie and Chow (1983). The fully implicit algorithm is second-order accurate in space and time. The approximation of integrals is based on the mid-point rule. Diffusion terms are approximated using second-order central differences, whereas advective fluxes are approximated based on blends between high-order upwind-biased schemes (e.g. QUICK), first order upwind and second order central differences schemes. Several turbulence models are implemented in the code, for the workshop computations, the standard k-ω turbulence model is applied. To account for the propeller rotation, the inertial frame of reference approach is taken. All equations are solved in an inertial coordinate system, the propeller, has to be moved.

3 NUMERICAL SETUP

3.1 Panel code computations

3.2 RANS computations

The propeller geometry provided by SVA was converted to a PARASOLID geometry and several grids were created using the grid generation software HEPRESS. The computational domain is shown in Fig. 1. Details of the Surface Grid can be found in Fig. 2. The computational domain was approximated by a cylinder with a radius of one propeller diameter D_P. The cylinder extended two propeller diameters upstream of and three propeller diameters downstream of the propeller for the open water test case. The cylinder radius was increased to 1.32 D_P for the velocity field test case.

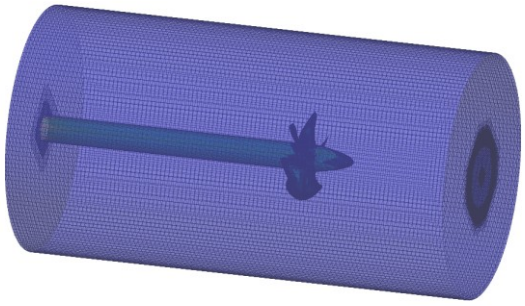

Figure 1: Domain for FreSCo

The computational grid size ranged from about 2.3 Million cells for the open water propeller test case to about 5.3 million cells for the velocity test case. The inflow boundary condition was set to v_∞. to match the advance coefficient J. The turbulence intensity was set to 10 %, the normalized eddy viscosity to 100. A no-slip boundary condition was set at the propeller blades, the cap and the shaft. A pressure boundary condition was set at the outlet and a slip wall boundary condition was set at the outer cylinder wall.

All calculations were performed using the standard $k-\omega$-model with wall functions.

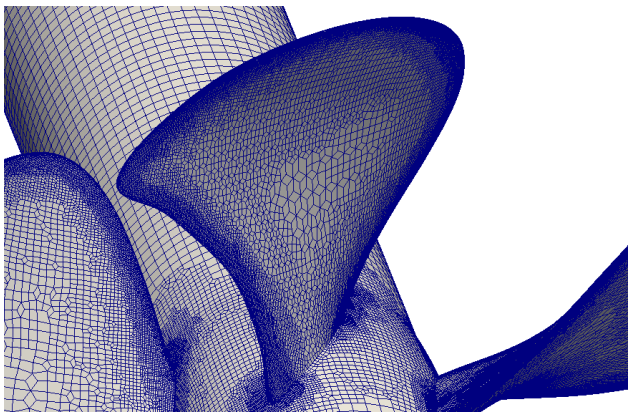

Figure 2: Blade Surface Representation for FreSCo

4 COMPUTATIONAL RESULTS

4.1 Open Water Curve

The results for the open water tests for 'PPB' and the RANS code are shown in Figure 3. Figure 4 compares 'PPB' and 'QCM'.

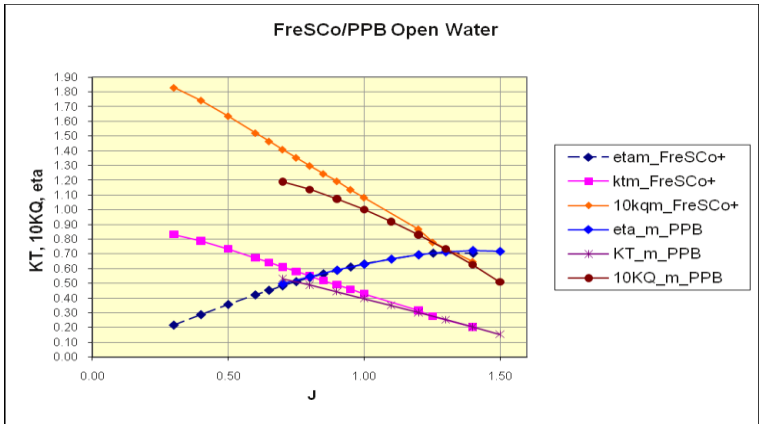

Figure 3: Open water diagram comparing FreSCo+ and PPB

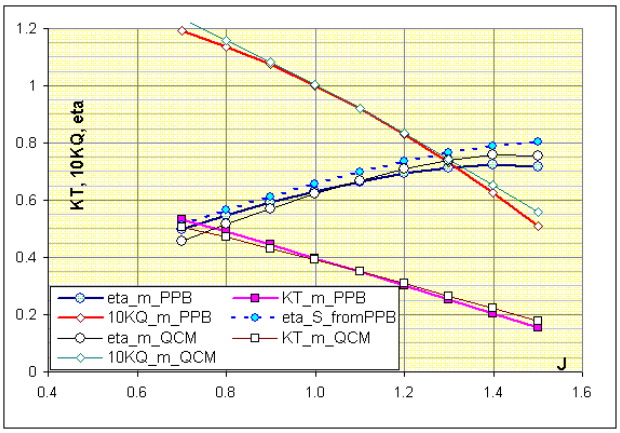

Figure 4: Open water diagram comparing QCM and PPB

4.2 Velocity field evaluation

In order to achieve thrust identity for the RANS computation the inflow velocity was increased to 7.451 m/s resulting in an advance coefficient of 1.296

In Fig. 5 the pressure distribution c_P on a propeller blade is shown. Fig 6. gives a representation of the surface streamlines using the Line Intergral Convolution (LIC) method for the shear stresses on the blade surface. c_P is defined as:

$$c_P = \frac{(p - p_0)}{0.5 \cdot \rho \cdot \left(V^2 + (2 \cdot \pi \cdot n \cdot r)^2\right)}$$

The Fig. 7 to 10 give a representation of the three dimensional flow effects. In Fig. 7 the iso surface of the pressure for $c_P = 0.05$ is shown. The iso surfaces for two different vorticity magnitude levels are shown in Figures 8 and 9. Figure 8 shows the vorticity in an XY plane. All pictures demonstrate that the tip vortices are captured.

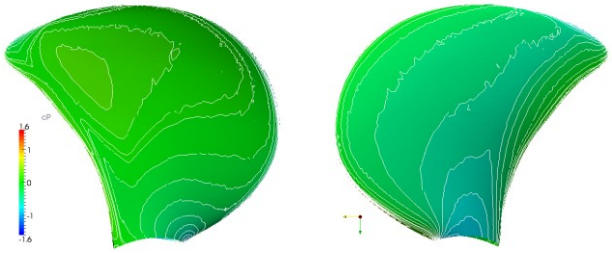

Figure 5: Pressure distribution c_P on a propeller blade

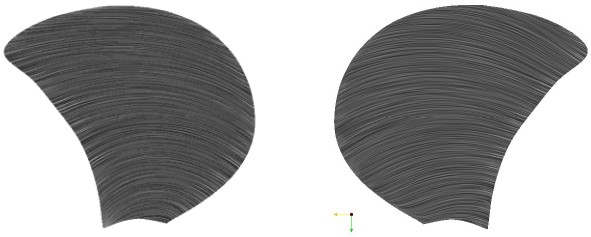

Figure 6: LIC on a propeller blade

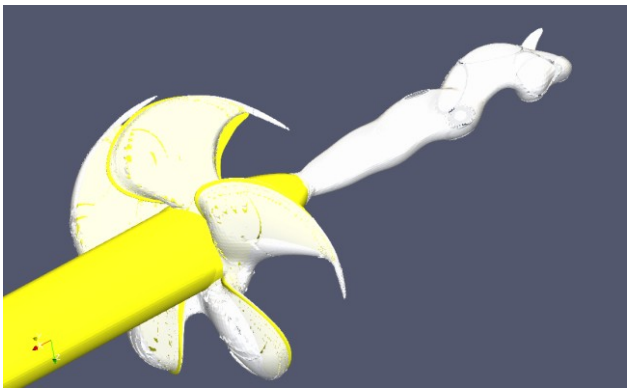

Figure 7: Pressure $c_{P=}$-0.05 iso surface

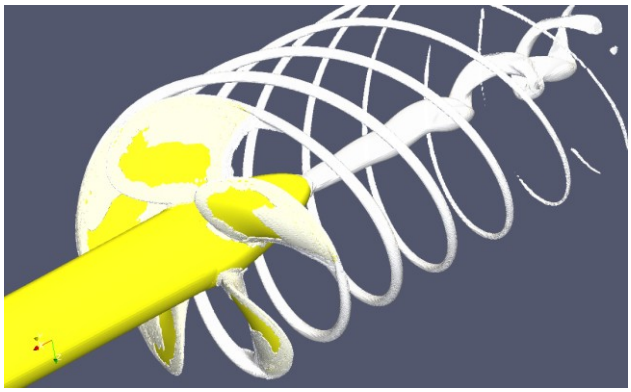

Figure 8: Vorticity magnitude=500 iso surface

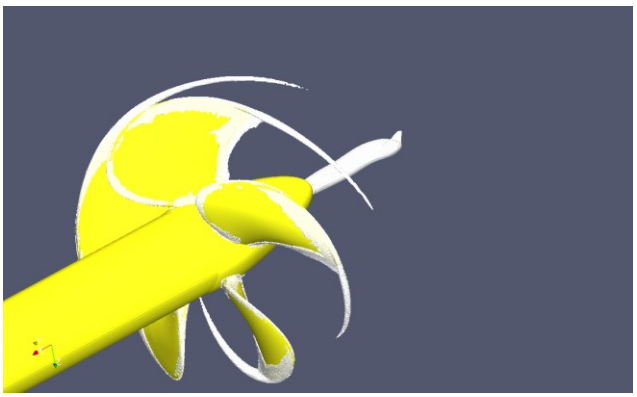

Figure 9: Vorticity magnitude=1000 iso surface

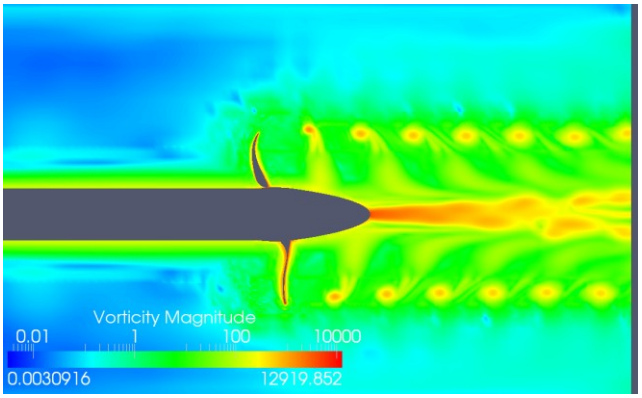

Figure 10: Vorticity Magnitude in a XY plane

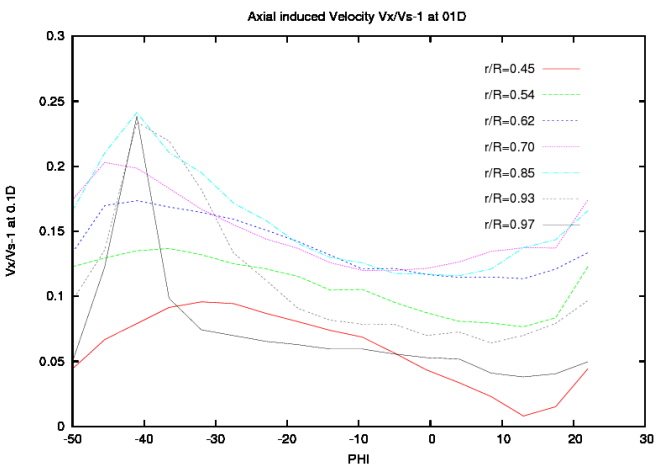

Figure 11: PPB results for the axial component (Vx/V-1) at 0.1 D behind the propeller plane

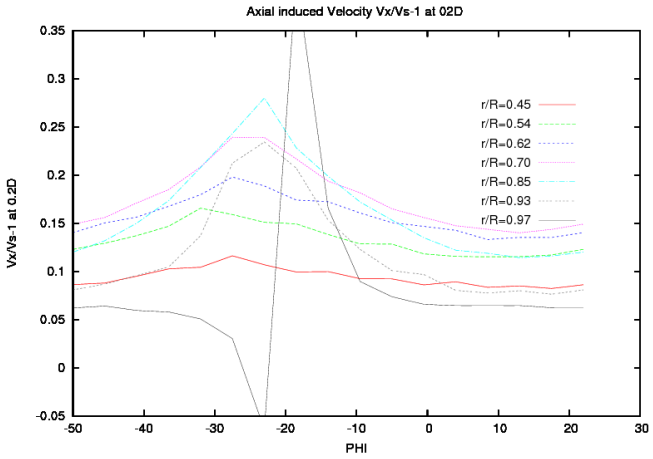

Figure 12: PPB results for Vx/V-1 at 0.2D

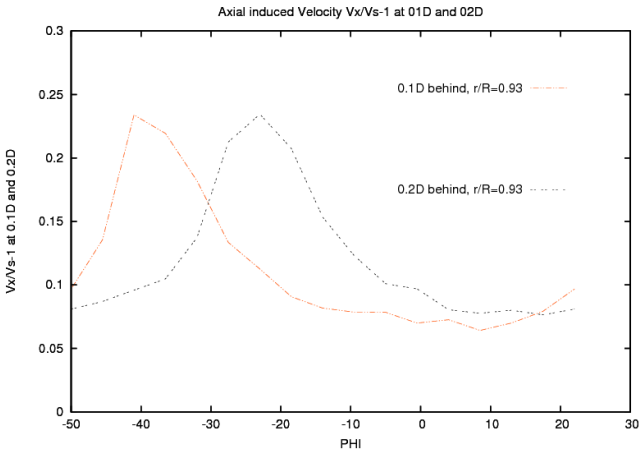

Figure 13: Comparing PPB results for planes 0.1D and 0.2D at r/R=0.93

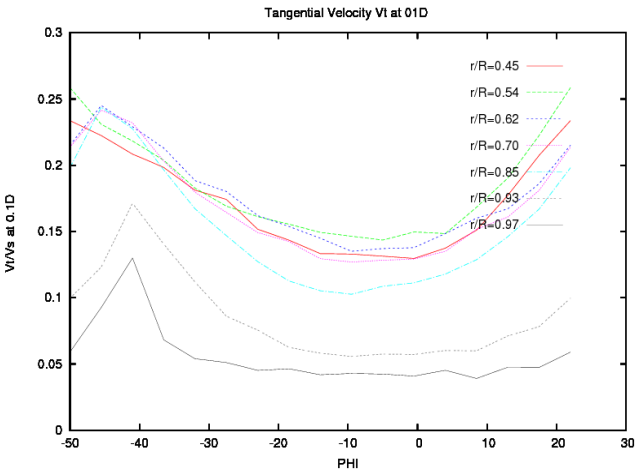

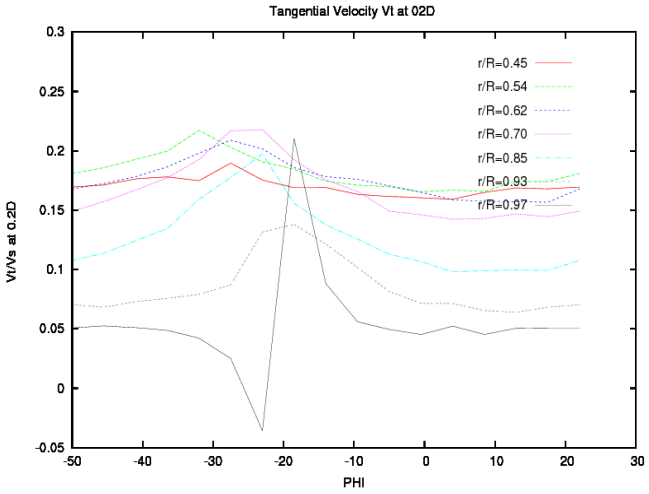

Figure 14: PPB results for the tangential component at 0.1D (above) and 0.2D (below)

To visualize the results of the Panel Method calculations we provide velocity components in form of x,y-diagrams. The horizontal axis describes the angular position and the vertical axis denotes the normalized magnitude of the axial or tangential component. For the axial component we were plotting and listing Vx/Vo-1 with Vo as undisturbed inflow, considering high axial induced velocity as positive.

The measuring points at 0° in the slipstream are considered fixed and the blade is considered moving (starting at PHI=0 and going to increasing PHI clockwise when looking from behind). Results for radial velocity are missing since they are not standard results from the PPB-method.

Figs. 11 to 14 show slipstream velocity results obtained for the two planes 0.1D and 0l.2 D behind the propeller, whereby Fig. 13 demonstrates the effect of changing planes for the axial component at r/R=0.93.

4.3 Cavitation

The cavitation computations for this paper were performed using QCM. Cavitation computations using FreSCo$^+$ can be found in the contributions from the group at TUHH.

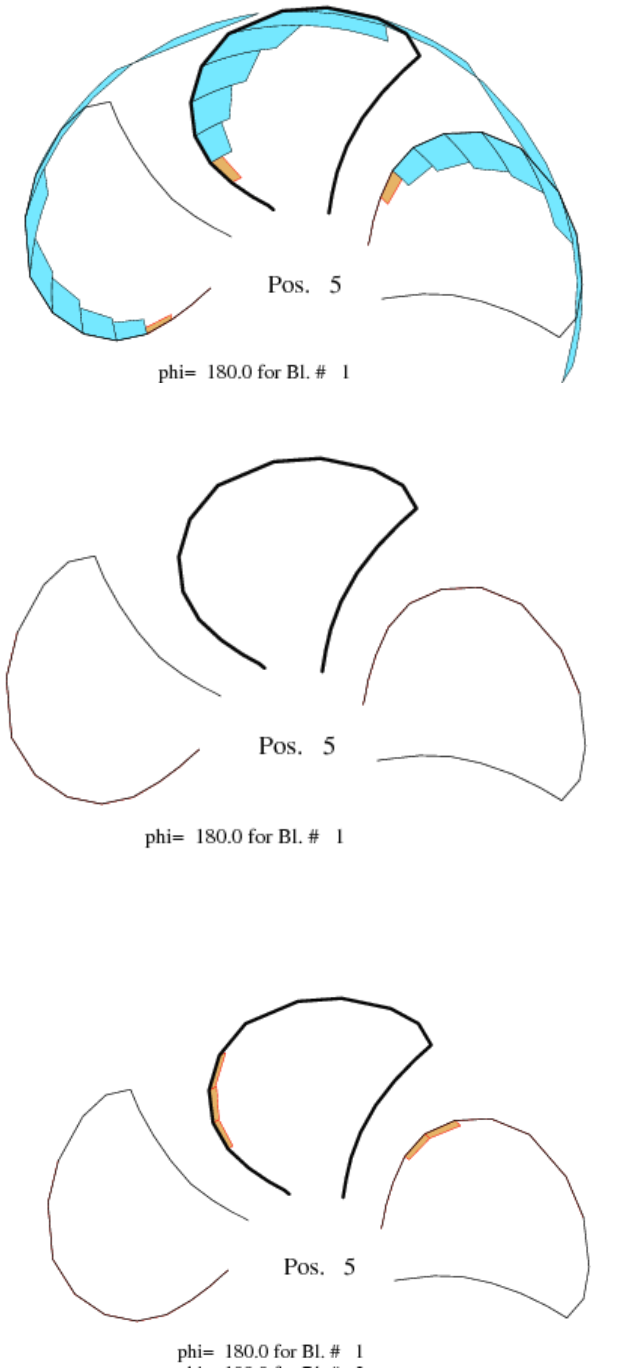

Figure. 15: QCM calculations for cavitation covering a) J=1.019, σ_n=2.024 (upper), b) J= 1.269, σ_n=1.424 (middle) and c) J=1.406 σ_n=2.00 (lower)

Fig. 15 shows calculatate cavitation extents. For the first case (J=1.019, σ_n=2.024) we found some suction side cavitation at the leading edge and some tendency to show a pronounced cavitating tip vortex. For the 2nd case (1.269, σ_n=1.424) no cavitation was detected. For the 3rd case (J=1.406, σ_n=2.00) we found some weakness to show pressure side cavitation (orange color). Figure 16: gives the estimated cavity profiles for J=1.019, σ_n=2.024 . The sections for the pressure side cavitation are hardly visible (Fig. 17) and it could probably not have shown up in the experiment.

REFERENCES

Hafermann, D. (2007). 'The New RANSE Code FreSCo for Ship Application', STG Jahrbuch 2007

HEXPRESS (2010), Full Hexahedral Grid Generation, http://www.numeca.be/index.php?id=29

Rhie, C.M. and Chow, W. L. (1983). 'A numerical study for the turbulent flow an isolated airflow with trailing edge separation', AIAA Journal,1983(**17**), pp. 1525

Streckwall, H. (1998): 'Hydrodynamic Analysis of Three Propellers Using a Surface Panel Method for Steady and Unsteady Inflow Conditions',22nd ITTC Propeller RANS/Panel Method Propeller Workshop, April 5.-6. 1998, Grenoble, France.

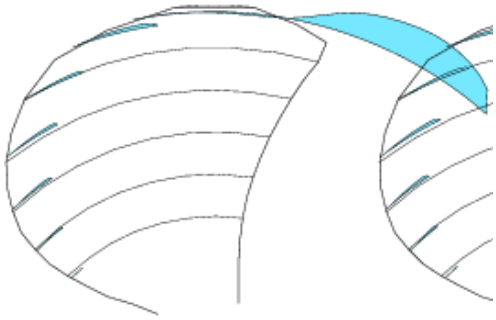

Figure 16: Estimated cavity profiles for case J=1.019, σ_n=2.024

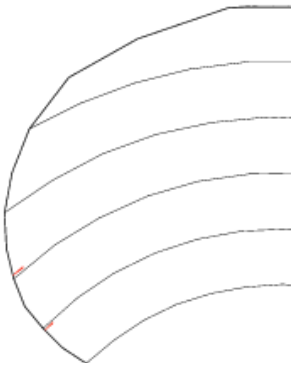

Figure 17: Estimated pressure side cavity profiles for case J=1.406, σ_n=2.00